Citation
Li, Z. and Chen, W. and Hao, H. and Yang, Q. and Fang, R. 2020. Energy absorption of kirigami modified corrugated structure. Thin-Walled Structures. 154: ARTN 106829. http://doi.org/10.1016/j.tws.2020.106829

Energy absorption of Kirigami modified corrugated structure

Zhejian Li[1], Wensu Chen[1]*, Hong Hao[1]*, Qiusong Yang[2], Rui Fang[2]

[1]*Centre for Infrastructural Monitoring and Protection*
School of Civil and Mechanical Engineering, Curtin University, Australia
[2]*School of Civil Engineering, Guangzhou University, China*

*corresponding author: wensu.chen@curtin.edu.au; hong.hao@curtin.edu.au

Abstract

In this study, a new Kirigami corrugated structure is designed. Dash lined cuts across each roll of corrugated structures are introduced and then folded inwards. The proposed Kirigami (cut and fold) modification provides extra vertical crushing resistance and constraints between the structure faces. Out-of-plane quasi-static tests are carried out for both conventional corrugated structures and Kirigami corrugated structures made of aluminium thin sheets. The numerical models with imposed imperfections are calibrated with the test data and then used for the dynamic crushing analysis of the structures under various loading rates. Key parameters such as initial peak force, average crushing resistance and energy absorption are compared among the conventional and Kirigami corrugated structures. Significant changes in deformation modes and great enhancement of energy absorption capacity under out-of-plane crushing are shown for the proposed Kirigami corrugated structures as compared to conventional corrugate structures. Furthermore, crushing resistance of the proposed Kirigami corrugated structure is less sensitive to imperfections. Great potential of the proposed Kirigami modification technique on corrugated structures is demonstrated with minimal change in its original manufacturing process but substantial enhancement in energy absorption capacities.

Keywords: Kirigami corrugated structure; energy absorption; dynamic crushing

1 Introduction

As one of the most common lightweight structures, corrugated sandwich structures are widely used in engineering practices including naval industries [1], aerospace [2], and protective structures for blast and impact attenuation [3-6]. Depending on the forms of the corrugation, corrugated structures can be categorized into triangular [2, 4, 5], trapezoidal [7, 8] and sinusoidal shapes [9, 10]. It was found that the corrugated structures have comparable shear strength in the longitudinal direction with honeycombs and greatly higher shear strength than other cellular sandwich structures such as diamond cores and foam cores [4]. Furthermore, corrugated sandwich structures show high bending resistance in the longitudinal direction [3] as well as excellent ventilation characteristics in reducing the humidity-retention issues which can be common for honeycombs and foams [2].

The flatwise-crushing behaviours of corrugated structures demonstrate less ideal characteristics for energy absorption. Rejab and Cantwell [2] found that under quasi-static flatwise crushing, non-uniform crushing resistances were observed through deformation for all triangular corrugated structures made of aluminium sheets, carbon fibre reinforced plastic (CFRP) and glass fibre reinforced plastic (GFRP). During deformation, the crushing resistance rises quickly at the initial stage, followed by a significant reduction. Kilicaslan et al [11] investigated the crushing responses of multilayer trapezoidal corrugated sandwich structures made of aluminium sheets. Significant increases in initial peak forces were observed in both experimental and FE results with strain rate from 10^{-1} to 40 s^{-1}. Furthermore, due to high initial peak crushing resistance and layer-by-layer deformation, all of the multi-layer specimens with interlayer plates demonstrated high fluctuations with multiple peaks throughout deformation under different strain rates. Similar high fluctuations in crushing resistances were also observed for graded multi-layer corrugated sandwich structures under impact [12]. These crushing characteristics of conventional triangular and trapezoidal corrugated structures under out-of-plane crushing, such as high initial peak force, strain rate sensitivity and fluctuating crushing resistance, are non-ideal for energy-absorbing purposes.

Over the last decade, various modifications have been implemented on conventional corrugated structures to improve their mechanical properties and energy absorption capabilities. A second-order hierarchical corrugated structure has been proposed to enhance the collapse strength of the conventional corrugated structure of the same mass [13]. Graded layers have been introduced to the multi-layer corrugated sandwich structure to improve the energy absorption and reduce the transmitted force under blast and high-speed impact. These graded corrugated structures can be achieved by either varying the layer thickness [14] or varying the geometrical corrugation on each layer [12, 15]. Furthermore, different staggering configurations have been investigated for multilayer corrugated structure, aiming to achieve higher energy absorption and lower initial peak crushing resistance without altering the geometry and thickness between layers [8, 11, 16, 17]. Stiffeners of different configurations have been added, connecting the two sidewalls of the triangular corrugated structure as well [18, 19]. Foam-filled corrugated structures have been extensively investigated under various loading conditions including dynamic loadings such as blast and impact [5, 9, 20-22]. As previously investigated, foam fillers can significantly enhance the energy absorption capacity of cellular structures without introducing higher initial peak force due to foam-wall interaction effect [23-25].

However, these previously proposed modification techniques have some drawbacks. Hierarchical corrugated structures require significant changes in manufacturing process than conventional corrugated structures and can be very costly to fabricate. Graded multi-layer corrugated structures may only be effective under high speed crushing and the enhancement in energy absorption is limited [12]. The increase in energy absorption of multi-layer corrugated structures with various staggering configurations is minimal, and the initial peak force is not eliminated [11, 16]. Added stiffeners may significantly increase the energy absorption of corrugated structure, but with initial peak force increased even greater. Furthermore, manufacturing cost and process can be increased due to welding or gluing of the additional stiffeners on corrugated structure. Foam-filled corrugated structures show ideal energy absorbing characteristics with significantly increased crushing resistance without inducing initial peak force [20]. However, the inserted metallic foam can be very expensive, and the extra bonding process is required. The filled metallic foam increases the overall mass of the structure as well. Therefore, new technique is required for enhancing the energy absorption capability and crushing performance of corrugated structures without greatly increasing the cost, manufacturing process and overall weight.

Origami and Kirigami modifications have been implemented on the conventional sandwich structures and energy absorbing structures recently. Origami structures are often referred to as three-dimensional structures folded from a flat sheet material without any cuts, whereas cuts are presented for Kirigami structures. Miura-type origami foldcore consists of rows of the zig-zag corrugated core have been proposed as a replacement of honeycomb structures in the aviation industry due to its ventability of the core [26]. Energy absorption and the crushing response of Origami structures were investigated under various loading rates [27, 28]. Different origami patterns have been introduced on tubular structures aiming to enhance their energy absorption capabilities and reduce the initial peak force by altering the collapsing modes with the origami patterns [29-33]. Moreover, Kirigami structures were investigated for their crushing responses [34-36]. The Kirigami concept is also used as a manufacturing technique for fabricating arbitrary shapes of honeycomb structures with high efficiency in the use of material [37].

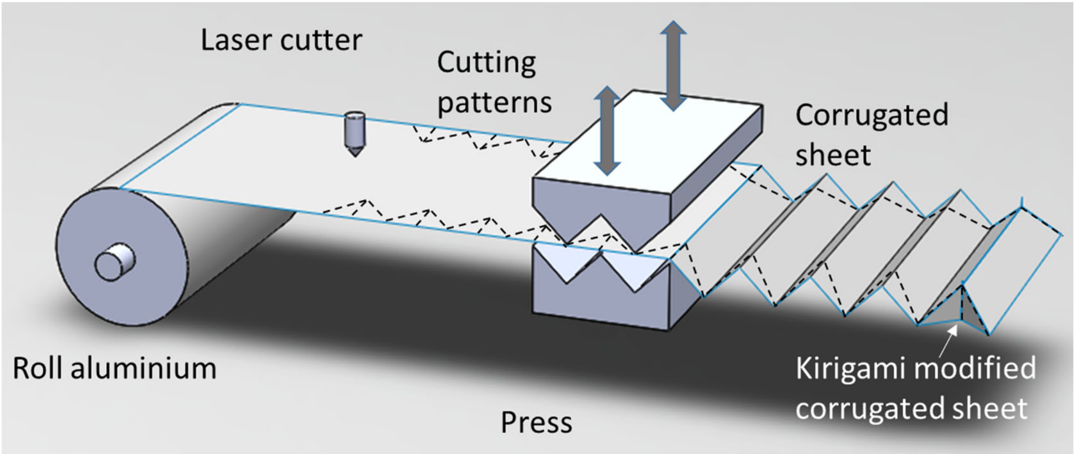

Figure 1. Proposed manufacturing process of Kirigami modified corrugated sheet

A Kirigami modification on conventional triangular and trapezoidal corrugated structures is proposed in this study. This modification includes a laser cutting process on sheet material before being pressed into the corrugated structure and the cut dash lines are later used as folding creases for Kirigami modification after the sheet is pressed into the corrugated structure as shown in Figure 1. This extra step of laser cutting has minimal influence on the conventional manufacturing process of corrugating structure presented by Wadley [3]. Therefore, the manufacturing cost of Kirigami modification of corrugated structure is low as compared to other modification methods such as hierarchical and stiffened corrugated structures. Furthermore, comparing to other modifications on corrugated structures including inserted stiffeners and foam fillers, the proposed Kirigami modifications bring no extra mass onto the corrugated structures. The Kirigami fold-ins are customizable, as the number and locations of cuts made on corrugated structures can vary in order to achieve different crushing response and energy absorption capacities.

In this study, energy absorption and crushing responses of Kirigami modified triangular and trapezoidal corrugated structures corresponding to quasi-static and dynamic out-of-plane deformation are investigated. Both Kirigami modified and conventional corrugated structures are crushed under quasi-static crushing. Numerical models are constructed and validated with the test data. Imperfections determined by Eigen mode analysis on cross-section of the structures are considered. The sensitivities to imperfections of the Kirigami modified and conventional corrugated structures are investigated and compared. Numerical simulations are carried out for Kirigami and conventional corrugated structures under dynamic crushing. Their energy absorption, peak force, average crushing resistance and densification strain are compared among the Kirigami modified and conventional corrugated structures with different imposed imperfections.

2 Geometry and specimen preparation

2.1 Geometry design

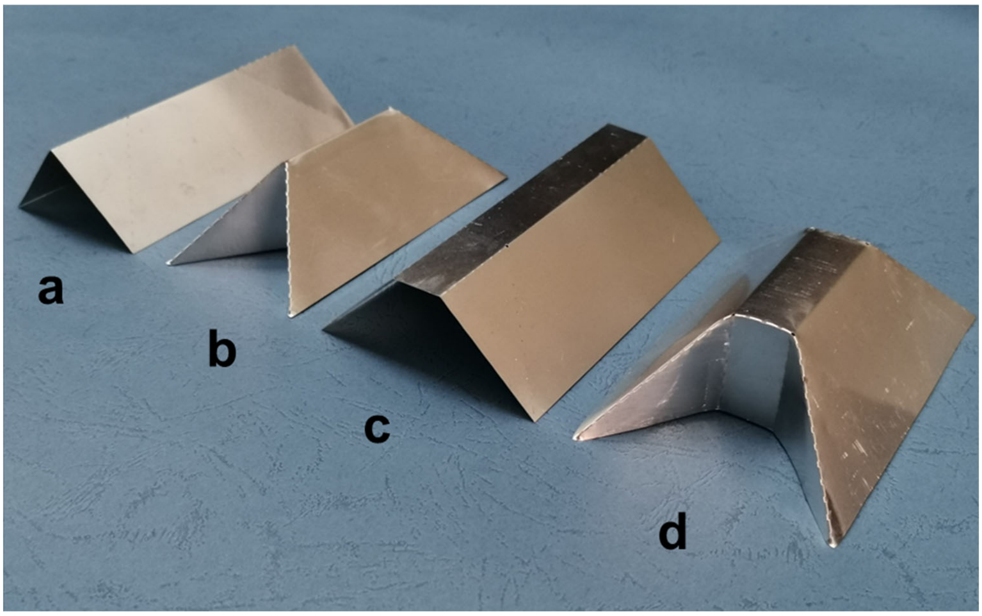

Figure 2. A unit cell of (a) Triangular corrugated structure; (b) Kirigami triangular corrugated structure; (c) Trapezoidal corrugated structure; (d) Kirigami trapezoidal corrugated structure; note: (a) and (c) have laser cut at two ends

As shown in Figure 2, two different conventional corrugated structures, i.e., triangular and trapezoidal, and their Kirigami variants were considered in this study. The material used for folding was Aluminium 1060 with the thickness, *t*, of 0.26 mm for all structures. The Kirigami modified corrugated structures were laser cut and then folded in at the two ends, as shown in dash lines in Figure 3. Both fold-in faces on Kirigami corrugated structure are perpendicular to the horizontal surface. The geometry of the Kirigami corrugated structure is defined by side face width, a, and structure height, h. Other geometric parameters used for designing the single cell Kirigami corrugated structure are shown in Figure 3 and can be expressed as follows:

$$c = h \tag{1}$$

$$b = 2\sqrt{a^2 - h^2} \quad \text{for triangular corrugated structure;}$$
$$b = 2\sqrt{a^2 - h^2} + e \quad \text{for trapezoidal corrugated structure} \tag{2}$$

$$d = \sqrt{a^2 + h^2} \tag{3}$$

$$\alpha = arcsin\,(\frac{h}{a}) \tag{4}$$

$$\beta = arctan\,(\frac{h}{a}) \tag{5}$$

$$\rho_r = \frac{2a\cdot t}{2\sqrt{a^2-h^2}\cdot h} \text{ for triangular corrugated structure;}$$
$$\rho_r = \frac{(2a+e)\cdot t}{(2\sqrt{a^2-h^2}+e)h} \text{ for trapezoidal corrugated structure} \tag{6}$$

where e is the top flat web width of trapezoidal corrugated structure; ρ_r is the relative volumetric density of the structure. Geometric parameters used in this study are listed in Table 1.

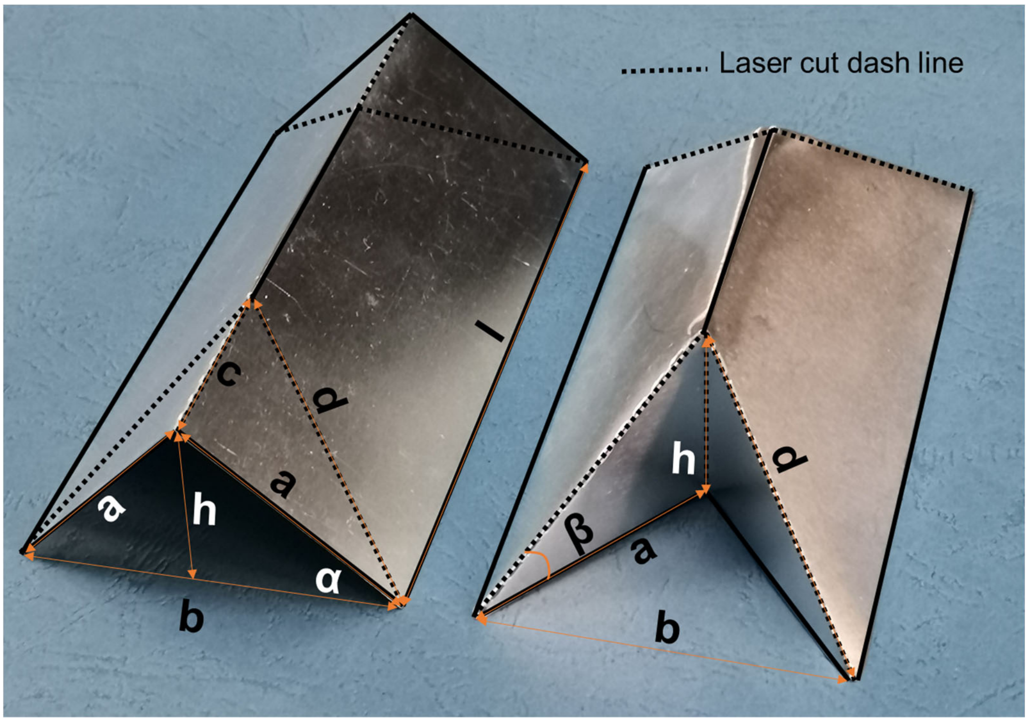

Figure 3. Geometric parameters of triangular corrugated structure and its Kirigami variant

Table 1. Geometric parameters used for corrugated structures and their Kirigami variants

a (mm)	b (mm)	c (mm)	d (mm)	h (mm)	l (mm)	α (degree)	β (degree)	e (mm)	t (mm)	ρ_r triangle/trapezoid
40	52.9	30	50	30	110	48.6	36.9	15	0.26	0.013/0.012

2.2 Laser cutting configurations

The Kirigami corrugated structures are achieved by folding parts of the sheet metal along the designed creases without using a die press, which can also be referred as Origami-based sheet bending. To achieve the easy folding of the sheet metal, dash lines also known as material discontinuity (MD) can be created using laser or water jet cutter according to Ablat and Qattawi [38]. It should be noted that the bending edges on conventional corrugated structures and the middle section of the Kirigami corrugated structures are not cut, as represented by solid black lines in Figure 3. To obtain the optimal MD design for the proposed Kirigami modification on corrugated structures, multiple sets of MD parameters were investigated on the same aluminium sheet used for specimen preparations. The aim is to achieve easy folding while maintaining the lowest cut-out area on aluminium sheet. Generic design parameters of MD and test sets of parameters are shown in Figure 4. Kerf of 0.1 mm was kept the same for all sets, which gives a kerf-sheet thickness ratio of 0.1/0.26 = 0.38, within the range of the recommended value from 0.2 to 0.5. The written label in Figure 4 represents the spacing and the MD length, for instance, "2/1" represents the cutting dash line consists of 2 mm of spacing for every 1 mm of MD length. After several folding tests on each set of parameters, the configuration of "3/1" (3 mm spacing with 1mm MD length) was selected out of the 16 sets due to the ease of folding and minimal cut out area on aluminium sheet. It was used for all Kirigami specimen preparations. Similarly, holes at the vertices of the bending edges, i.e., the corners on top of Kirigami modified corrugated structure, were cut for the ease of folding. Four different diameters of the holes including 0.5, 1, 1.5 and 2 mm were cut and tested for folding. 1 mm-diameter hole showed a similar effect with respect to the easy of folding as compared to 1.5 and 2 mm holes, therefore was used for specimen preparation in this study.

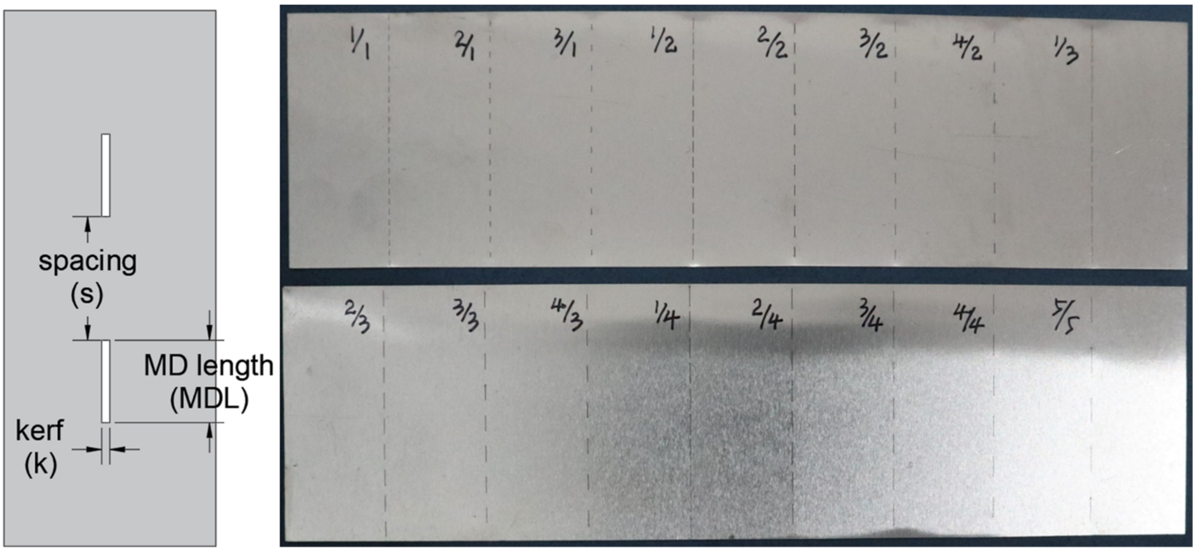

Figure 4. Design parameters of material discontinuity (MD) and tested MD configurations on aluminium sheets (s/MDL in mm)

3 Quasi-static crushing

3.1 Experiment tests

3.1.1 Experimental setup

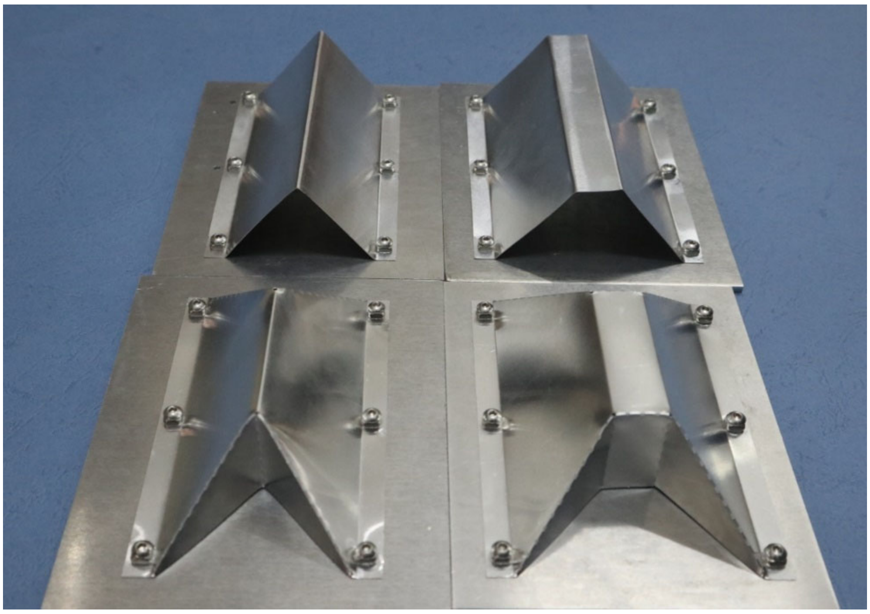

Figure 5. Setup of conventional corrugated structures (back row) and Kirigami modified corrugated structures (front row)

Four configurations of specimens were prepared manually using Al 1060 aluminium sheet. The dash lines were only cut along the folding edges for Kirigami modified sections at two ends. No cut was made on the conventional corrugated structures or the middle section of Kirigami corrugated structures, consistent with the current manufacturing process for conventional corrugated structures where the corrugation of sheet metal is achieved by die pressing [3]. Due to the size of the crushing disk on the testing machine, the specimens used in this study were short and was a single row of corrugated structure. The prepared specimens were then bolted down on to a 3 mm-thick aluminium alloy plate made of Al 5083, as shown in Figure 5. Six bolts with square nuts, which were flushed with the bottom edges of the corrugated structures, were used for fixing for each specimen. All the four corrugated structures had the same height of 30 mm, while the widths are 52.9 and 67.9 mm for triangular and trapezoidal corrugated structures, respectively. The bolted specimens were then crushed under a constant speed of 2 mm/min until about 25 mm of displacement. As the specimens were bolted to the base plate, further crushing will lead to contact between bolts and crushing disc, therefore result in incorrect force measurements. Both the crushing and supporting disks on the compressive test machine had diameter of 150 mm.

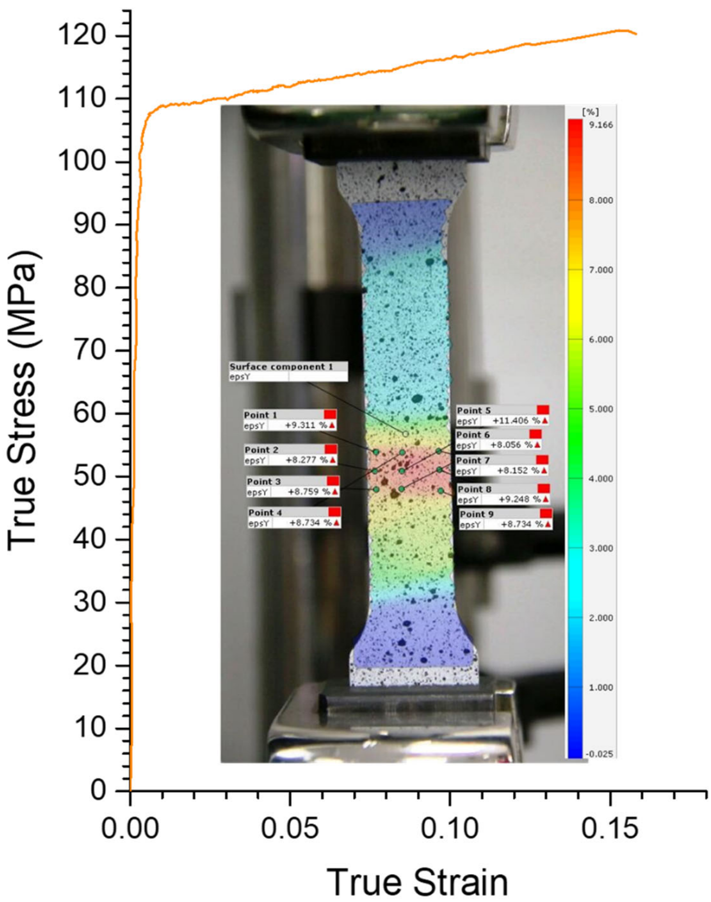

Figure 6. True stress-strain curve of aluminium 1060 sheet material where strain is measured using DIC analysis.

The tensile test of Al 1060 sheet was carried out in accordance with ASTM E-8M [39] under quasi-static loading condition with a constant loading rate of 1mm/min. The true stress-strain curve of Al 1060 sheet is shown in Figure 6, where the engineering strain was firstly measured using Digital Image Correlation (DIC) technique and then converted to true strain. The density of Al 1060 and Al 5083 is 2710 and 2660 kg/m^3 respectively, and their yield strength is 110 MPa and 215 MPa [40].

3.1.2 Test results

The load-displacement curves of conventional and Kirigami triangular/ trapezoidal corrugated structures under quasi-static crushing are shown in Figure 7 (a) and (b), respectively. Three curves are included for each type of conventional corrugated structures, including two specimens of different deformation modes and one specimen with laser cut material discontinuity (MD) but not folded, which are marked as "01", "02", and "laser cut" in Figure 7, respectively. The laser-cut pattern is the same as the Kirigami modification but without two ends folded-in. This is to test the influence of the laser cut MD on the crushing response of conventional corrugated structures. The load-displacement curves of both Kirigami modified corrugated structures are consistent among different tests, therefore, a representative curve is shown in Figure 7 (a) & (b) for Kirigami triangular and trapezoidal corrugated structure. The experimental data from the tests are listed in Table 2 and the parameters are defined as follows:

$$P_{ave} = \frac{\int_0^{\delta_d} P(\delta)\, d\delta}{\delta_d} \quad \text{where } \delta_d = 25mm \tag{7}$$

$$P_{ave,0-10mm} = \frac{\int_0^{10} P(\delta)\, d\delta}{10} \tag{8}$$

$$EA = P_{ave} \cdot \delta_d \tag{9}$$

$$SEA = \frac{EA}{m} \tag{10}$$

P_{ave} is the average crushing force from 0 to 25 mm of displacement except for trapezoidal corrugated 01, as a sharp rise in crushing force is observed at around 23.5mm displacement indicating the densification (δ_d) is reached. $P_{ave,0\text{-}10mm}$ is the average crushing force from 0 to 10 mm displacement, as crushing resistance remains at a low level for conventional corrugated structure during this first stage regardless of the overall deformation mode. P_{peak} is the peak crushing force during the deformation. EA and SEA are the energy absorption and specific energy absorption of the structure throughout the deformation, where *m* is the mass of the structure. The uniformity ratio, *U*, is defined as the ratio of the peak to average crushing resistance for each specimen.

Table 2. Experimental data of conventional and Kirigami modified corrugated structures under quasi-static crushing

Corrugated structure	Specimen	P_{ave} (N)	$P_{ave,0\text{-}10mm}$ (N)	P_{peak} (N)	$U=P_{peak}/P_{ave}$	EA (J)	SEA (J/g)
Triangular	01	229	111	728	3.18	5.66	0.916
	02	75	65	246	3.28	1.81	0.292
	with laser cut	82	72	156	1.90	2.03	0.328
Kirigami triangular		753	597	990	1.31	18.63	3.016
Trapezoidal	01	150	127	250	1.67	3.58	0.488
	02	251	88	491	1.96	6.20	0.845
	with laser cut	82	77	185	2.26	2.03	0.277
Kirigami trapezoidal		926	769	1221	1.32	22.89	3.121

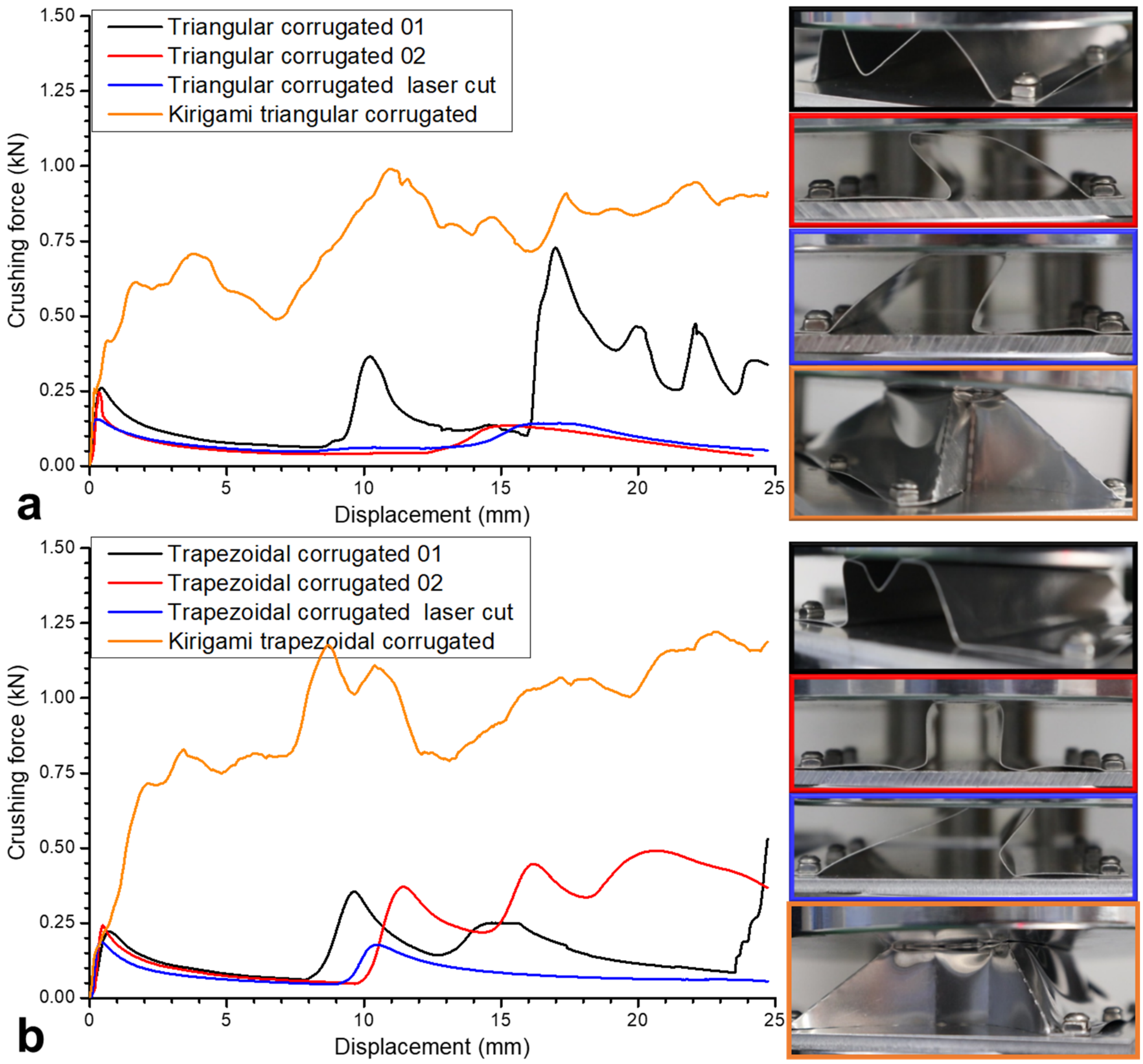

Figure 7. Load-displacement curves of conventional and Kirigami (a) triangular; (b) trapezoidal corrugated structures and their associated deformation modes under quasi-static crushing

3.1.3 Comparison and analysis

As shown in Figure 7, distinct differences in crushing response can be observed between conventional corrugated structures and the corresponding Kirigami modified corrugated structures. High initial peak force followed by a quick reduction in crushing resistance is shown in Figure 7 for both triangular and trapezoidal corrugated structures regardless of deformation modes. During the first 10 mm of crushing, similar crushing responses are shown for conventional corrugated structures regardless of the differences in deformation modes. The similarity in crushing resistance at the initial stage among these structures is because of the almost identical development of plastic hinge lines, i.e., the same amount of plastic hinge lines are formed and similar bending deformation propagates along the faces of the corrugated structures regardless of the deformation modes. However, in some cases, additional plastic hinge lines and extra support are created in the later crushing stage once the middle portion is in contact with the base plate, therefore resulting in higher crushing resistance. For instance, the triangular corrugated structure 01 marked out in the black square in Figure 7 (a) has a higher crushing resistance than the other two cases in the later stage, because the middle section provides additional resistance when it is in contact with the base. These different deformation modes are caused by different imperfections induced during the specimen preparation. In summary, both configurations of the conventional corrugated structures have non-ideal characteristics for energy absorption, as concluded in [41], since the crushing resistances are either too low or inconsistent throughout the deformation.

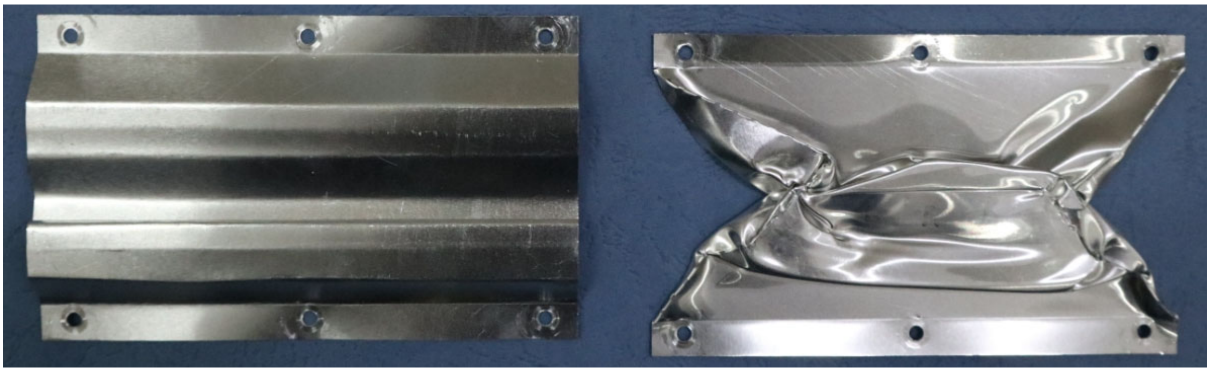

Figure 8. Comparison of deformation mode of triangular corrugated structure 01 and Kirigami triangular corrugated structure

With the Kirigami modification, both triangular and trapezoidal corrugated structures demonstrated enhanced crushing responses for energy absorption. No initial peak is observed during the crushing process. In fact, even the overall peak force during the whole process of crushing is only about 1.31 times of the average crushing force. As for comparison, this ratio can reach up to 3.28 for conventional corrugated structure depending on the deformation modes. Secondly, the crushing resistance is much more constant throughout deformation with less fluctuation. As shown in Figure 7, crushing resistance of the both Kirigami corrugated structures fluctuated slightly around the average for the majority of the crushing process. More importantly, the crushing resistances are significantly enhanced for both shapes of corrugated structures with the Kirigami modification, especially during the first half of the crushing until around 10 mm of displacement. For instance, the crushing resistance increased to more than 10 times for Kirigami triangular corrugated structure as compared to conventional triangular corrugated structure 02. Similarly, the overall average crushing force increased 3.7 times after the Kirigami modification, and 8.7 times during the first 10 mm of crushing compared to the conventional trapezoidal corrugated structure 02, which has the highest energy absorption.

The fold-ins on Kirigami modified corrugated structure significantly changed the deformation modes of the conventional corrugated structure. As discussed, deformation of the conventional corrugated structure is mostly contributed by the propagation of plastic hinge lines. Nearly no deformation is observed apart from the bending at the plastic hinge lines as shown in Figure 8. With the Kirigami modification, the vertical triangle shaped folded web sections provide lateral support as well as constraints to the side faces, resulting in a complete buckling on the web sections and the large plastic deformation on the connecting side faces. The vertical web section provides significant increase in energy absorption, similar grid structure can be found in [42, 43]. As shown in Figure 7, the deformation mostly concentrated on the top near the contact between the structure and crushing disk. Due to the increasing cross-section of the fold-ins from top to bottom, the crushing resistance of Kirigami modified corrugated structure increases slightly with respect to crushing distance. Different from some of the modification methods such as foam infill and varying staggering configurations, this proposed Kirigami modification completely altered the deformation modes of corrugated structure and therefore significantly improved its energy absorption capacities without introducing additional weight.

3.2 Finite element analysis

3.2.1 Finite element modelling

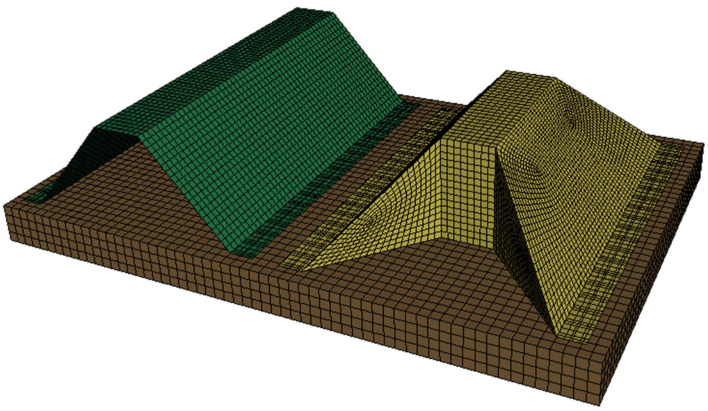

Figure 9. Numerical model of trapezoidal corrugated structure (L) and Kirigami modified corrugated structure (R)

Numerical simulations were carried out in LS-DYNA. As shown in Figure 9, shell element was used for modelling the thin-walled corrugated structures, whereas rigid solid elements were used for modelling crushing and supporting plates. The six bolted fixings were modelled by constraining all six degrees of freedom of the nodes on corrugated structures at corresponding locations. Al 1060 thin sheet made of the corrugated structure was modelled using *MAT_24 PIECEWISE LINEAR PLASTICITY and the material parameters of Al 1060 were obtained from the measured data in Figure 6. The strain rate effect was not considered in this FE model, as aluminium alloy is insensitive to strain rate [8, 44]. The friction coefficient of 0.25 was applied between all interfaces [35]. By conducting mesh convergence test, the mesh size of 2 mm is selected for the FE analysis in this study and the accuracy of the FE model has been verified with test data as well. To ensure the accuracy of the quasi-static simulation and computational efficiency, the crushing speed was ramped during the first 50 ms to 0.5m/s and kept constant until 25 mm of displacement [45]. The ratio between total kinetic energy and total internal energy was also checked to be less than 0.05 during the crushing process [35, 46]. The crushing force in FE simulations was measured from the top impact end.

3.2.2 Imperfections in numerical model

To accurately model the crushing responses of the corrugated structures, especially during the initial stage, imperfections were imposed into numerical models to account for the inevitable manufacturing errors in practice. Some assumptions were made for the efficiency in modelling the imperfections. In this study, first four basic buckling modes (I to IV) obtained from Eigen value analysis on the cross-section of the corrugated structures were used for defining the shapes of four modes of imperfections as shown in Figure 10, similar to [19]. No imperfection was imposed along the longitudinal direction for each mode, and the mix-mode of the imperfections are not considered. It should be noted that the amplitude of initial deformation shown in Figure 10 are amplified, the actual imperfections were small. The maximum amplitude of these imperfections was estimated to be 0.5 mm between two farthest points from the side face for all of the modes, where one example of mode II is illustrated in Figure 10. This value was measured and averaged from side faces of multiple specimens. The deviated positions of the nodes on the cross-section of the corrugated structures are then calculated and the numerical models are constructed based on these deviations from nominal geometry. No imperfection was considered on the fold-ins at two ends on Kirigami modified corrugated structures. Numerical simulations of the structures without any imperfections were also carried out as a comparison to illustrate the sensitivity of different corrugated structure to imperfections.

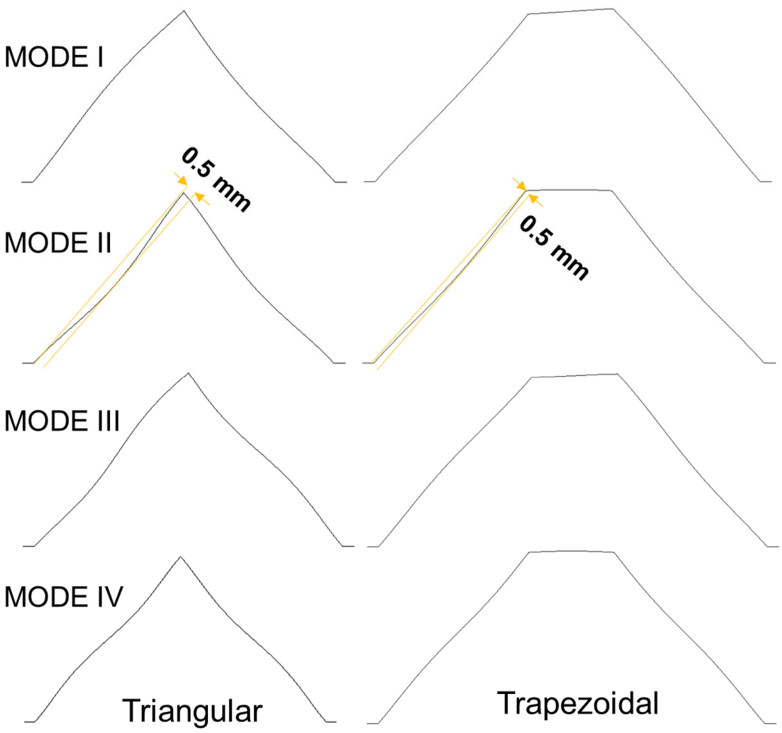

Figure 10. Imperfections imposed on side faces of triangular and trapezoidal corrugated structures based on buckling mode; Note: the imperfections are not to scale

3.2.3 Results and discussions

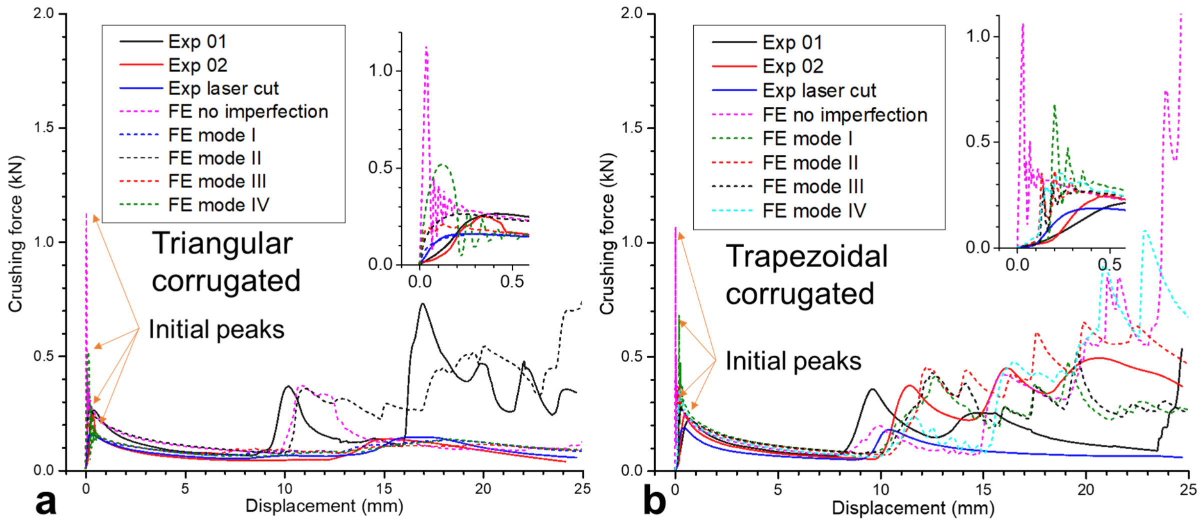

Figure 11. Load-displacement curves of (a) triangular; (b) trapezoidal corrugated structures with different imperfections under quasi-static crushing

The comparisons of load-displacement curves from test and finite element analysis are shown in Figure 11 and Figure 12. For conventional corrugated structures shown in Figure 11, their out-of-plane crushing responses are strongly dependent on the imperfections, especially for the initial peak crushing force, as imperfections can greatly affect the buckling force of the plate.

For instance, for both triangular and trapezoidal corrugated structures, the numerical model of structure without any imperfections leads to a significantly higher initial peak force up to 5 times than that from tests. For the numerical model of the triangular corrugated structure with mode IV imperfections and trapezoidal corrugated structure with mode I imperfections, marked in green dash lines, their initial crushing resistance is around twice of the test data (solid lines), while models with other modes of imperfections are relatively well matched with the test data in terms of the initial peak force. Similar crushing responses are shown after the initial stage till around 10 mm of displacement regardless of the deformation modes and imperfections, indicating the imperfection greatly affects the initial crushing responses, but its effect diminishes in the late crushing stage. During the late crushing stage, the plastic hinge lines which occur across the whole length of the corrugated structure propagate similarly despite the difference in the initial crushing force. Once the deformed section on the corrugated structures are in contact with the supporting plate after crushing deformation reaches 10 mm, the crushing responses become different again depending on the deformation modes. The crushing responses of FE models with different modes of imperfections are illustrated with different colours, in which the FE results that are closest to the test results are marked with similar colours as the test results, but with different line patterns. For instance, FE model of triangular corrugated structure with mode II imperfection is illustrated with black dash line, corresponding to the black solid line of the test results of Exp 01, as they show similar crushing responses. Similarly, FE model of the structure with mode III imperfection is illustrated with red dash line, corresponding to test results of Exp 02 as shown in Figure 11 (a). Same colour coding is used for the trapezoidal corrugated structure in Figure 11 (b).

Comparing to the conventional corrugated structures, Kirigami modified corrugated structures are less sensitive to imperfections under quasi-static loading condition. As shown in Figure 12, the crushing responses of the test results and FE results with or without imperfections are similar for both Kirigami modified structures. In general, the overall crushing responses including initial peak force, fluctuation during crushing are matched relatively well regardless of the imposed imperfections in FE models. This is different from the conventional corrugated structures where a significantly higher initial peak force is observed on FE models of the structures without imperfections. This low sensitivity to imperfections for Kirigami variants is caused by the changing of deformation modes, from shape-dependent global plate buckling in one direction only presented in the conventional corrugated structure to more localised deformation as more constraints are provided by the fold-ins to the side faces. The Kirigami trapezoidal corrugated structure shows a slightly more sensitivity on the modes of imperfections than its triangular counterpart. For the Kirigami triangular corrugated structure, the overall fluctuations in crushing resistance are similar for FE models of structures with different modes of imperfections, whereas the Kirigami trapezoidal corrugated structures with mode II and IV imperfections experience a slightly larger fluctuation as shown in Figure 12 (b).

Slight differences of initial peak forces are also observed in the Kirigami modified corrugated structures with different imperfections, even though the differences among these results are greatly reduced as compared to the conventional corrugated structures. For instance, FE models of structures with mode I and III imperfections show slightly lower initial peak force as compared to the other three FE results for both the triangular and trapezoidal Kirigami corrugated structures. The initial peak forces from the models with these two modes (I &III) are closer to the test values. It is also worth noting that the initial stiffness of FE results is higher than that of the test data. This is because some slight gaps are presented between the web sections on Kirigami corrugated structure and supporting plate due to manufacturing errors. During the initial crushing process up to 2 mm, the gaps gradually closes and the crushing force rises. Therefore, the value of the initial peak force is similar between the test and FE results, but the stiffness is different.

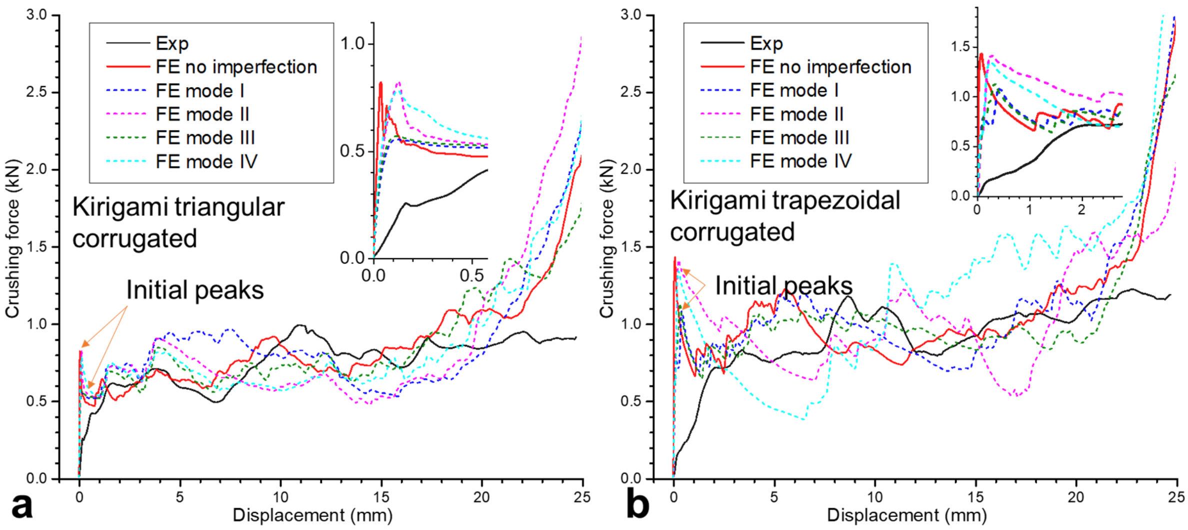

Figure 12. Load-displacement curves of Kirigami (a) triangular; (b) trapezoidal corrugated structures with different imperfections under quasi-static crushing

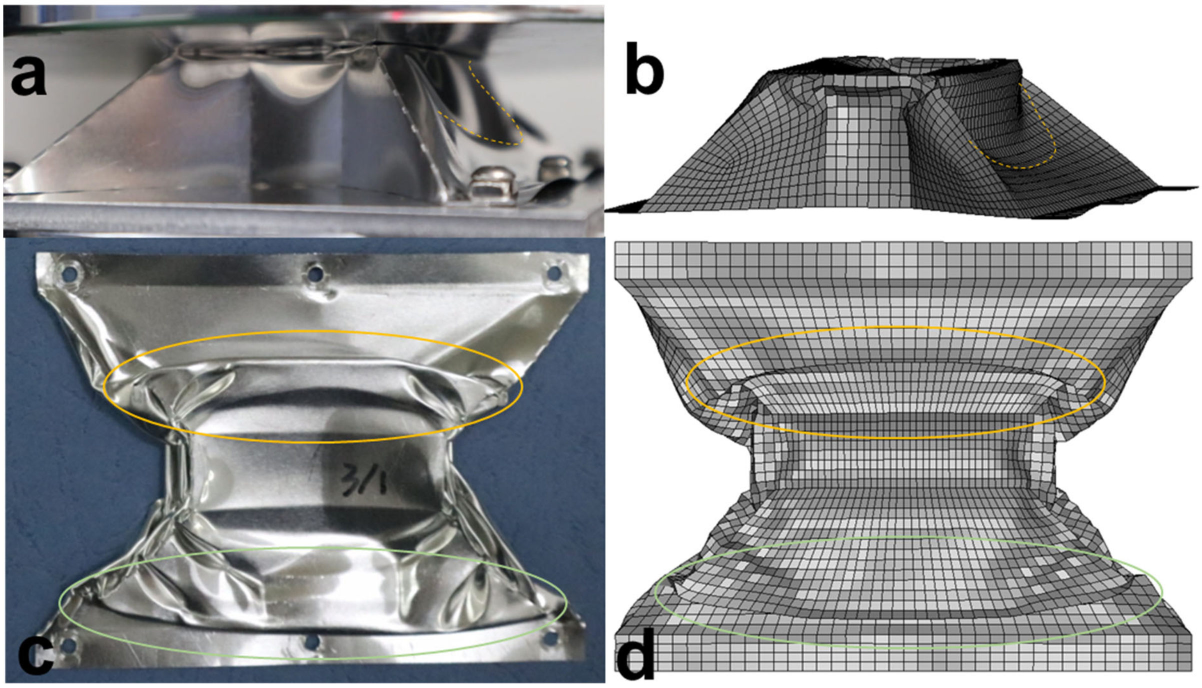

Figure 13. Comparison of deformation modes of FE (with mode III imperfection) and test results of Kirigami trapezoidal corrugated structure

The deformation modes from FE simulations are reasonably matched with the test results. Comparison of the deformation modes from the test and FE results of structures with the most well matched imperfection mode III of Kirigami modified corrugated structure is shown in Figure 13 a-d. As shown, the fold-ins experienced local buckling and multiple folding during the crushing of the structure, whereas the side faces buckled globally along a curve marked out in yellow dash lines. Due to the imperfections induced during the preparation of the specimens, the global buckling on two side faces are not symmetric as marked out in yellow and green circles in Figure 13 c. The numerical model with mode III imperfections captured this as well. The buckling locations are different on two sides of the faces, one closes to the top and the other one closes to the bottom. However, this asymmetry of damage on Kirigami modified corrugated structure caused by imperfections has minimal effect in overall crushing resistance and energy absorption.

To summarize, the crushing responses of conventional and Kirigami modified corrugated structures are matched between tests and FE models of structures with imperfections. The responses of both conventional triangular and trapezoidal corrugated structures are strongly dependent on the modes of imperfections, as significant differences in initial peak force and deformation modes are shown among the FE model of structures with different imposed imperfections. The Kirigami modified triangular and trapezoidal corrugated structures are less sensitive to imperfections due to their different deformation modes.

4 Dynamic crushing

4.1 Deformation mode comparison

Comparisons of deformation modes of the corrugated structures and their Kirigami variants under quasi-static and 10 m/s crushing are shown in Figure 14 and Figure 15. The FE models of structures with imperfection modes (i.e. basic mode I to IV) are shown for both quasi-static and 10 m/s crushing in Figure 14 and Figure 15. For the triangular corrugated structure, the deformation modes show minimal overall change for the models under loading rate of 10 m/s for lower modes of imperfections. However, the local deformation near the impacting plate is much more obvious under dynamic crushing. This is caused by the inertia effect of the structure and leads to the increase in initial peak force under dynamic loading. The triangular corrugated structure with mode IV imperfections has more plastic hinge lines under loading rate of 10 m/s than that under quasi-static crushing, which leads to a high spike in crushing resistance once the middle parts on the side faces are in contact with the base plate. This significant increase in crushing resistance can be observed at later stage of the load-displacement curve shown in section 4.2. The Kirigami modified triangular corrugated structures show similar overall deformation modes under the two crushing speeds. Similarly, more localized deformation near the impacting plate can be observed, and leads to an increase in crushing resistance under dynamic crushing.

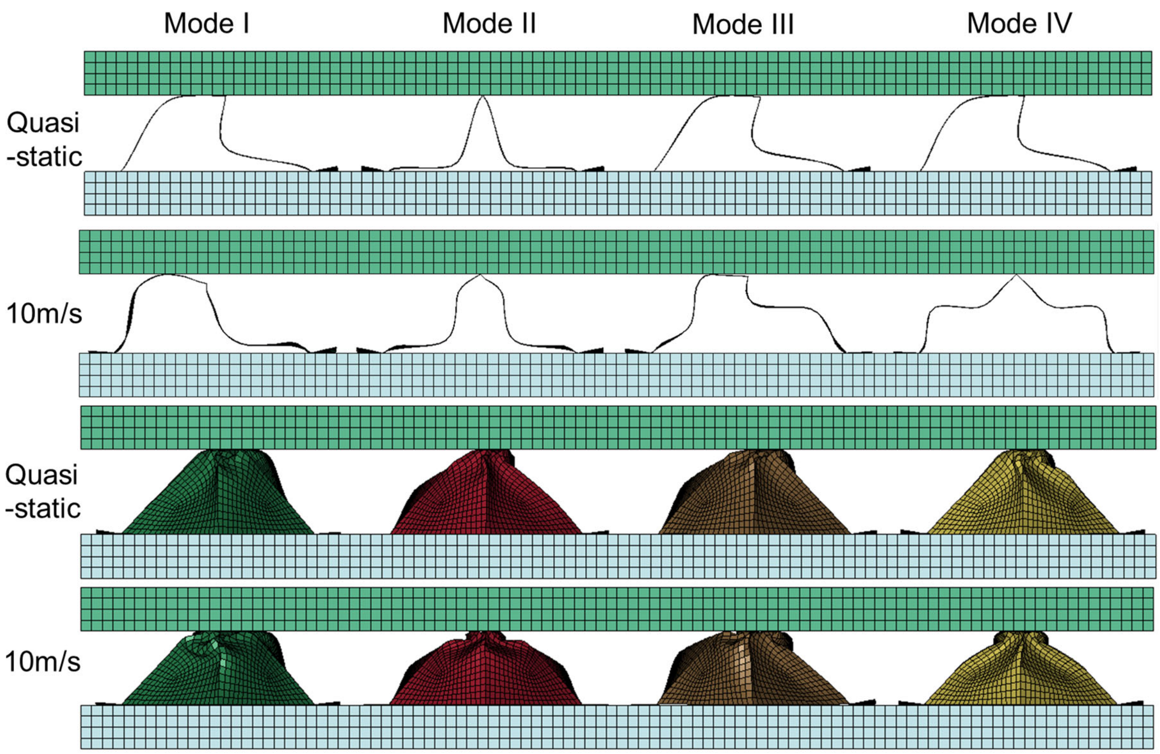

Figure 14. Deformation mode comparison of FE models with different imperfections for triangular corrugated structure and its Kirigami variant under quasi-static and 10 m/s crushing

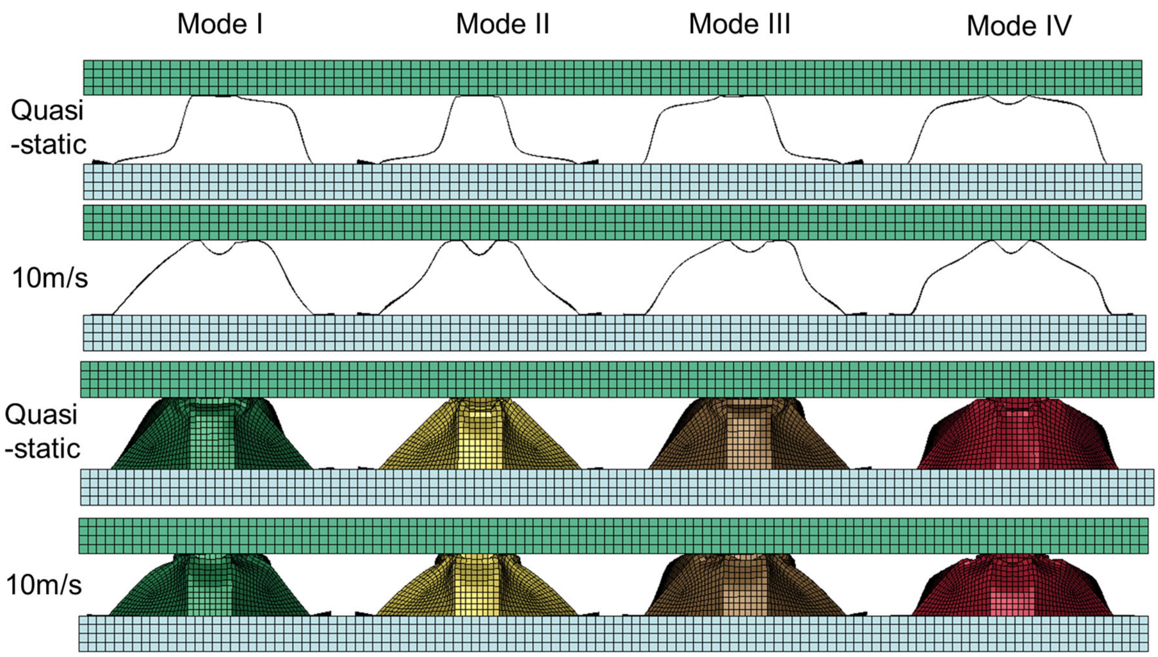

Figure 15. Deformation mode comparison of FE models with different imperfections for trapezoidal corrugated structure and its Kirigami variant under quasi-static and 10 m/s crushing

The trapezoidal corrugated structure becomes less sensitive to different modes of imperfections under 10 m/s crushing as compared to the quasi-static crushing. Different from the triangular corrugated structure, in trapezoidal corrugated structure, the two side faces are connected by a flat web. Under impact, the two side faces tend to bend downwards and the top edges are pushed closer, leading to the formation of plastic bending hinge line in the middle of the flat web in-between the two side faces. Under quasi-static crushing, there is sufficient time for the side faces to deform, resulting in the minimal deformation on the top flat web. Thus, the deformation of trapezoidal corrugated structure is mostly dependent on the induced imperfections under quasi-static crushing. With Kirigami modification on trapezoidal corrugated structure, however, similar overall deformation modes are demonstrated for both quasi-static and 10 m/s crushing, with more localised deformation towards the top crushing plate.

4.2 Load-displacement curves

The load-displacement curves of FE models with different imperfections under 10 m/s crushing are shown in Figure 16. Different from the quasi-static crushing shown in section 3.2.3 where the significant influence of imperfections is shown for the conventional corrugated structures, the overall crushing responses of conventional corrugated structures are similar regardless of the different imperfections, despite some differences still exist in part of the crushing process. For instance, the fluctuation levels are similar for each type of corrugated structure with different imperfections. However, as shown in the figure, some differences are still observed, especially in the responses of the triangular corrugated structure due to its different deformation modes. FE model of this structure with mode IV imperfection shows a high spike at the later stage of the crushing. As shown in Figure 14, additional plastic hinge lines on side faces of FE model with mode IV imperfection lead to additional contacts to the base plate at the later stage of crushing, which causes higher inertia stabilizing effect under dynamic loads. Furthermore, high initial peak impacting force is observed on all four types of corrugated structures, but both the Kirigami modified structures show reduced initial peak force than their conventional corrugated counterparts, implying less sensitive to the loading rate. The value of initial force remains similar for most considered structures with different imperfections except the trapezoidal corrugated structure. The FE model of the trapezoidal corrugated structure without imperfection has a significantly higher initial peak force than the models with four configurations of imperfections. For the trapezoidal corrugated structure without imperfection (i.e. perfectly flat top web), the contact area is larger and the impact duration is much shorter as compared to the structures with imperfections (i.e. the top webs are not perfectly flat). This lead to an increase in contact stiffness in penalty-based contact in LS-DYNA [47], thus the spike in contact force [48]. Similar huge spike in initial contact force at impact end was also observed on the closed top truncated pyramid structure with a perfectly flat top surface under dynamic crushing in a previous study [34].

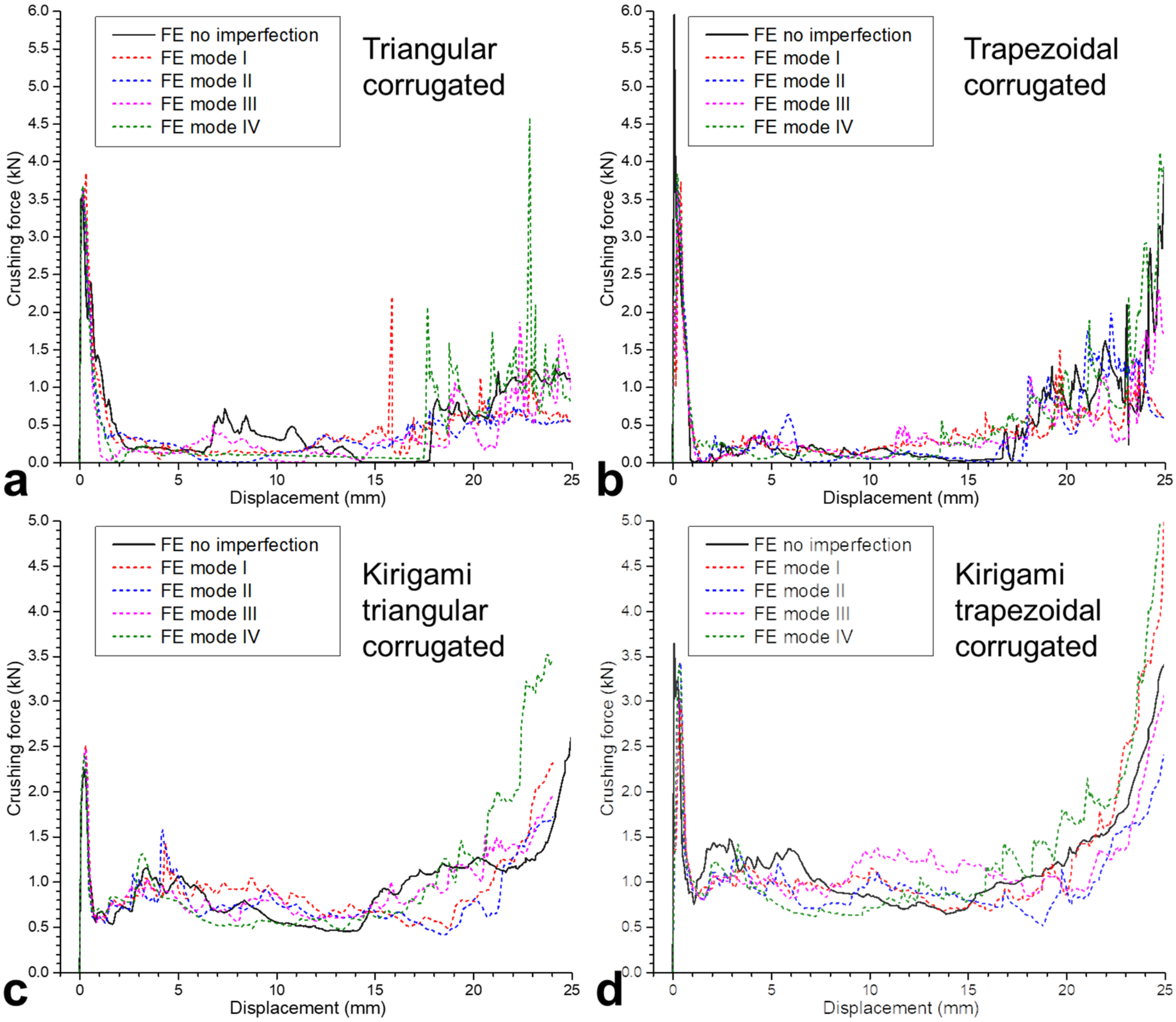

Figure 16. Load-displacement curves of FE models with different modes of imperfections under 10 m/s crushing; Note: crushing force is measured from the impact end

The average crushing resistance of Kirigami modified corrugated structures are greatly higher than that of the respective conventional corrugated counterparts under dynamic crushing. Similar to quasi-static crushing, low fluctuation throughout the crushing and low sensitivity to imperfections can be observed for both the Kirigami modified structures under dynamic crushing. For instance, as shown in Figure 16, the crushing resistance of Kirigami triangular corrugated structure varies from approximately 0.5 to 1.5 kN for all the considered structures with different types of imperfections throughout the deformation, excluding the initial peak section, whereas the range for the conventional triangular corrugated structure is from 0 to 4.5 kN. Similar behaviours can be observed for the Kirigami trapezoidal corrugated structure and the conventional trapezoidal corrugated counterpart. Zero crushing force can be observed during a portion of the crushing process for both the conventional corrugated structures with no imperfections under dynamic loading, for instance, triangular corrugated structure without imperfection during crushing from 15 to 18 mm of displacement. This zero crushing force is caused by snap-through instability of the structure, meaning the structure upon reaching the critical force can rapidly transform into another state without further applying force [49]. This phenomenon can be commonly found in many structures [50, 51] including corrugated structure [19]. However, this phase is not ideal for energy-absorbing purpose as no crushing resistance is provided during the process of snap-through. Overall, despite the high spike of initial peak force, the web structures in Kirigami modification lead to a significant enhancement in energy absorption over the conventional corrugated structures under quasi-static and dynamic out-of-plane crushing, and more stable crushing resistance as well as less sensitive to loading rate.

4.3 Peak force and energy absorption

Comparisons of peak force and average crushing force among the four types of corrugated structures with different configurations of imperfections under quasi-static loading and 10 m/s crushing are shown in Figure 17. It should be noted that the peak force is measured as the maximum force during crushing before reaching densification state where a consistent sharp rise in crushing resistance occurs. Two distinct trends can be observed for the conventional corrugated structures and the Kirigami modified corrugated structures. For both triangular and trapezoidal corrugated structures, significant increases in peak force up to 20 times are shown when the crushing speed is 10 m/s as compared to that from the quasi-static crushing. The corresponding increases in peak force of the Kirigami modified triangular and trapezoidal corrugated structures are approximately 2 times.

The average crushing force for all structures increased slightly with the increase of crushing speeds. As discussed in section 4.1, more localised deformation is presented under dynamic crushing which is caused by the inertia effect of the structure. Furthermore, the adjacent faces provide additional support to the structure under dynamic loading due to inertial stabilization effect, result in a higher crushing resistance. It is noted that the average crushing force of the Kirigami modified corrugated structures greatly exceeds their conventional corrugated counterparts. Their average crushing forces are also more consistent under both the static and dynamic loading conditions, indicating the modified Kirigami corrugated structures have better energy absorbing performances than the conventional ones.

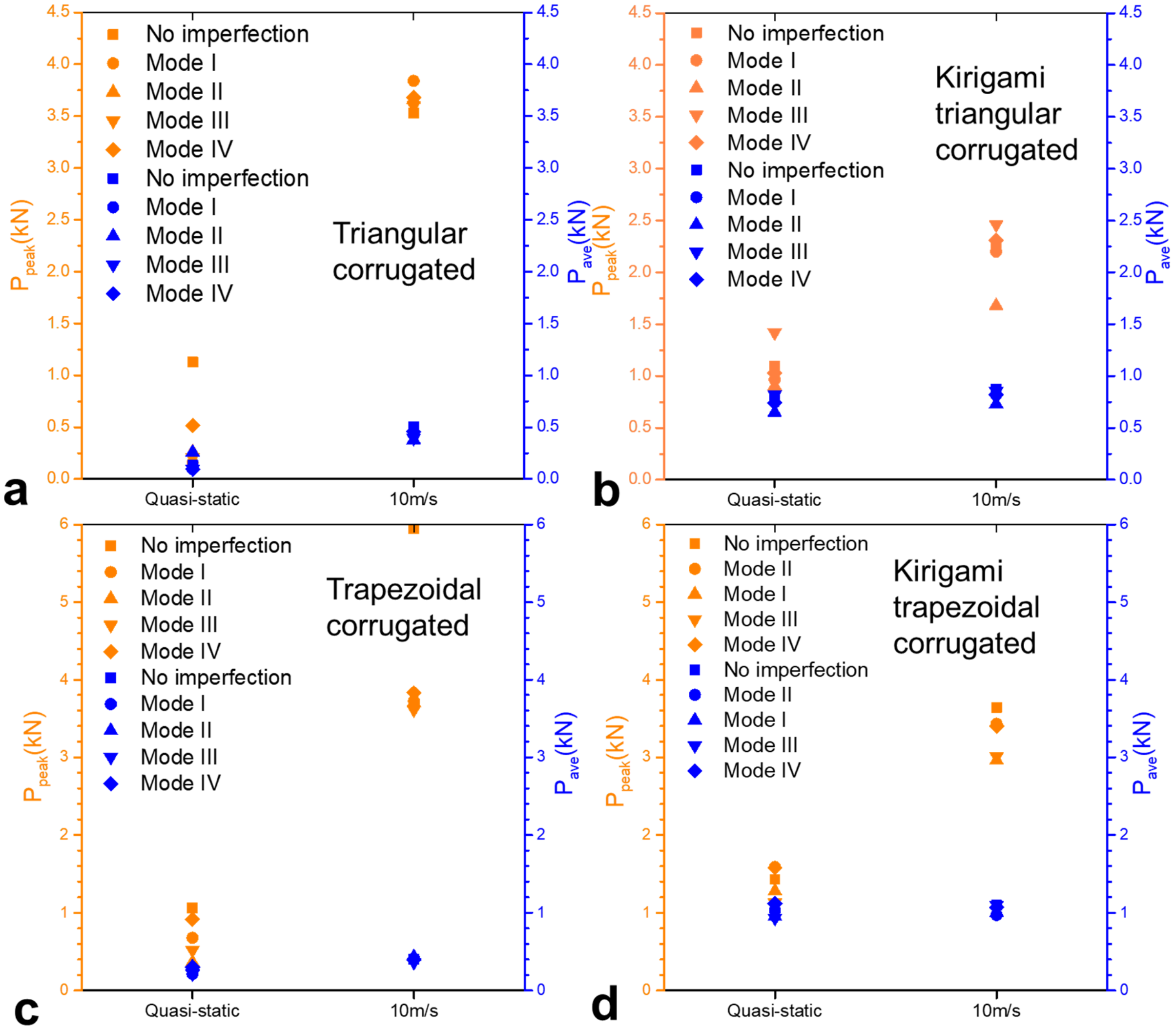

Figure 17. FE results of peak (orange) and average (blue) crushing force of (a) Triangular corrugated structure; (b) Kirigami modified triangular corrugated structure; (c) Trapezoidal corrugated structure; (d) Kirigami modified trapezoidal corrugated structure, under quasi-static and 10 m/s crushing; Note: crushing force is measured from the impact end

5 Conclusion

Kirigami modification is proposed for conventional triangular and trapezoidal corrugated structures. The web sections of the Kirigami modified corrugated structures provide extra supports and constraints to the adjacent side faces under out-of-plane crushing. Quasi-static crushing tests are carried out on fully bolted structures. The proposed Kirigami modified corrugated structures outperform the conventional corrugated structures with low initial peak force, uniform crushing resistance and less sensitivity to initial imperfections. The average crushing resistance increases up to 10 times as compared to the conventional corrugated structures. Numerical simulations are carried out with the assumed imperfections based on buckling mode analysis. The numerical results of these structures agree well with the quasi-static test data, depending on the assumed initial imperfections. Dynamic crushing responses of the proposed structures are also numerically investigated. Despite having a rise in the initial peak force under 10 m/s crushing, the overall crushing responses of Kirigami modified corrugated structures show superior characteristics than the conventional corrugated counterparts. With the Kirigami modification, the structures are less sensitive to loading rates, have significantly larger average crushing resistance, enhanced energy absorption capacity, and more consistent crushing responses than the conventional corrugated structures. These indicate the potential applications of the proposed Kirigami modifications for enhancing the energy absorption capacity of corrugated structures under out-of-plane crushing. The proposed Kirigami corrugated structure could be used as the core of sandwich structure in energy absorption applications such as impact attenuator and blast mitigation cladding.

Acknowledgements

The authors acknowledge the support from Australian Research Council via Discovery Early Career Researcher Award (DE160101116).

Reference

[1] L. St-Pierre, V.S. Deshpande, N.A. Fleck, The low velocity impact response of sandwich beams with a corrugated core or a Y-frame core, International Journal of Mechanical Sciences, 91 (2015) 71-80.

[2] M.R.M. Rejab, W.J. Cantwell, The mechanical behaviour of corrugated-core sandwich panels, Composites Part B: Engineering, 47 (2013) 267-277.

[3] H.N. Wadley, Multifunctional periodic cellular metals, Philos Trans A Math Phys Eng Sci, 364 (2006) 31-68.

[4] F. Côté, V.S. Deshpande, N.A. Fleck, A.G. Evans, The compressive and shear responses of corrugated and diamond lattice materials, International Journal of Solids and Structures, 43 (2006) 6220-6242.

[5] B. Russell, A. Malcom, H. Wadley, V. Deshpande, Dynamic compressive response of composite corrugated cores, Journal of mechanics of materials and structures, 5 (2010) 477-493.

[6] G.K. Schleyer, M.J. Lowak, M.A. Polcyn, G.S. Langdon, Experimental investigation of blast wall panels under shock pressure loading, International Journal of Impact Engineering, 34 (2007) 1095-1118.

[7] V. Rubino, V.S. Deshpande, N.A. Fleck, The dynamic response of clamped rectangular Y-frame and corrugated core sandwich plates, European Journal of Mechanics - A/Solids, 28 (2009) 14-24.

[8] C. Kılıçaslan, M. Güden, İ.K. Odacı, A. Taşdemirci, The impact responses and the finite element modeling of layered trapezoidal corrugated aluminum core and aluminum sheet interlayer sandwich structures, Materials & Design, 46 (2013) 121-133.

[9] M. Yazici, J. Wright, D. Bertin, A. Shukla, Experimental and numerical study of foam filled corrugated core steel sandwich structures subjected to blast loading, Composite Structures, 110 (2014) 98-109.

[10] E. Magnucka-Blandzi, K. Magnucki, L. Wittenbeck, Mathematical modeling of shearing effect for sandwich beams with sinusoidal corrugated cores, Applied Mathematical Modelling, 39 (2015) 2796-2808.

[11] C. Kılıçaslan, M. Güden, İ.K. Odacı, A. Taşdemirci, Experimental and numerical studies on the quasi-static and dynamic crushing responses of multi-layer trapezoidal aluminum corrugated sandwiches, Thin-Walled Structures, 78 (2014) 70-78.

[12] B.T. Cao, B. Hou, H. Zhao, Y.L. Li, J.G. Liu, On the influence of the property gradient on the impact behavior of graded multilayer sandwich with corrugated cores, International Journal of Impact Engineering, 113 (2018) 98-105.

[13] G.W. Kooistra, V. Deshpande, H.N. Wadley, Hierarchical corrugated core sandwich panel concepts, Journal of applied mechanics, 74 (2007) 259-268.

[14] L. Zhang, R. Hebert, J.T. Wright, A. Shukla, J.-H. Kim, Dynamic response of corrugated sandwich steel plates with graded cores, International Journal of Impact Engineering, 65 (2014) 185-194.

[15] Z. Zhang, H. Lei, M. Xu, J. Hua, C. Li, D. Fang, Out-of-plane compressive performance and energy absorption of multi-layer graded sinusoidal corrugated sandwich panels, Materials & Design, 178 (2019).

[16] S. Hou, C. Shu, S. Zhao, T. Liu, X. Han, Q. Li, Experimental and numerical studies on multi-layered corrugated sandwich panels under crushing loading, Composite Structures, 126 (2015) 371-385.

[17] C. Shu, S. Zhao, S. Hou, Crashworthiness analysis of two-layered corrugated sandwich panels under crushing loading, Thin-Walled Structures, 133 (2018) 42-51.

[18] T. Tran, Crushing and theoretical analysis of multi-cell thin-walled triangular tubes under lateral loading, Thin-Walled Structures, 115 (2017) 205-214.

[19] S.C. Wehmeyer, Designing Novel Cell-Based Structures for Energy Absorption, in, University of California, Santa Barbara, 2019.

[20] L.L. Yan, B. Yu, B. Han, C.Q. Chen, Q.C. Zhang, T.J. Lu, Compressive strength and energy absorption of sandwich panels with aluminum foam-filled corrugated cores, Composites Science and Technology, 86 (2013) 142-148.

[21] B. Yu, B. Han, C. Ni, Q. Zhang, C. Chen, T. Lu, Dynamic crushing of all-metallic corrugated panels filled with close-celled aluminum foams, Journal of Applied Mechanics, 82 (2015) 011006.

[22] Y. Cheng, M. Liu, P. Zhang, W. Xiao, C. Zhang, J. Liu, H. Hou, The effects of foam filling on the dynamic response of metallic corrugated core sandwich panel under air blast loading – Experimental investigations, International Journal of Mechanical Sciences, 145 (2018) 378-388.

[23] Z. Li, W. Chen, H. Hao, Dynamic crushing and energy absorption of foam filled multi-layer folded structures: Experimental and numerical study, International Journal of Impact Engineering, 133 (2019) 103341.

[24] W. Chen, T. Wierzbicki, Relative merits of single-cell, multi-cell and foam-filled thin-walled structures in energy absorption, Thin-Walled Structures, 39 (2001) 287-306.

[25] A.G. Hanssen, M. Langseth, O.S. Hopperstad, Static and dynamic crushing of circular aluminium extrusions with aluminium foam filler, International Journal of Impact Engineering, 24 (2000) 475-507.

[26] S. Heimbs, Foldcore sandwich structures and their impact behaviour: an overview, in: Dynamic failure of composite and sandwich structures, Springer, 2013, pp. 491-544.

[27] J.M. Gattas, Z. You, Quasi-static impact of indented foldcores, International Journal of Impact Engineering, 73 (2014) 15-29.

[28] J.M. Gattas, Z. You, The behaviour of curved-crease foldcores under low-velocity impact loads, International Journal of Solids and Structures, 53 (2015) 80-91.

[29] J. Ma, D. Hou, Y. Chen, Z. You, Quasi-static axial crushing of thin-walled tubes with a kite-shape rigid origami pattern: Numerical simulation, Thin-Walled Structures, 100 (2016) 38-47.

[30] J. Ma, H. Dai, M. Shi, L. Yuan, Y. Chen, Z. You, Quasi-static axial crushing of hexagonal origami crash boxes as energy absorption devices, Mechanical Sciences, 10 (2019) 133-143.

[31] K. Yang, S. Xu, J. Shen, S. Zhou, Y.M. Xie, Energy absorption of thin-walled tubes with pre-folded origami patterns: Numerical simulation and experimental verification, Thin-Walled Structures, 103 (2016) 33-44.

[32] C. Zhou, B. Wang, J. Ma, Z. You, Dynamic axial crushing of origami crash boxes, International Journal of Mechanical Sciences, 118 (2016) 1-12.

[33] C. Zhou, Y. Zhou, B. Wang, Crashworthiness design for trapezoid origami crash boxes, Thin-Walled Structures, 117 (2017) 257-267.

[34] Z. Li, W. Chen, H. Hao, Crushing behaviours of folded kirigami structure with square dome shape, International Journal of Impact Engineering, 115 (2018) 94-105.

[35] R.K. Fathers, J.M. Gattas, Z. You, Quasi-static crushing of eggbox, cube, and modified cube foldcore sandwich structures, International Journal of Mechanical Sciences, 101-102 (2015) 421-428.

[36] T. Nojima, K. Saito, Development of newly designed ultra-light core structures, JSME International Journal Series A Solid Mechanics and Material Engineering, 49 (2006) 38-42.

[37] K. Saito, F. Agnese, F. Scarpa, A Cellular Kirigami Morphing Wingbox Concept, Journal of Intelligent Material Systems and Structures, 22 (2011) 935-944.

[38] M.A. Ablat, A. Qattawi, Investigating the design and process parameters of folded perforated sheet metal, The International Journal of Advanced Manufacturing Technology, 102 (2019) 615-633.

[39] ASTM, E8M-04 Standard Test Methods for Tension Testing of Metallic Materials (Metric) 1, ASTM international, 2004.

[40] Z. Li, W. Chen, H. Hao, Functionally graded truncated square pyramid folded structures with foam filler under dynamic crushing, Composites Part B: Engineering, (2019) 107410.

[41] G. Lu, T. Yu, Energy Absorption of Structures and Materials, Woodhead publishing limited, Cambridge England, 2003.

[42] H. Fan, Y. Luo, F. Yang, W. Li, Approaching perfect energy absorption through structural hierarchy, International Journal of Engineering Science, 130 (2018) 12-32.

[43] W. Hong, H. Fan, Z. Xia, F. Jin, Q. Zhou, D. Fang, Axial crushing behaviors of multi-cell tubes with triangular lattices, International Journal of Impact Engineering, 63 (2014) 106-117.

[44] Y. Zhang, M. Lu, C.H. Wang, G. Sun, G. Li, Out-of-plane crashworthiness of bio-inspired self-similar regular hierarchical honeycombs, Composite Structures, 144 (2016) 1-13.

[45] S.P. Santosa, T. Wierzbicki, A.G. Hanssen, M. Langseth, Experimental and numerical studies of foam-filled sections, International Journal of Impact Engineering, 24 (2000) 509-534.

[46] A. Baroutaji, M.D. Gilchrist, D. Smyth, A.G. Olabi, Analysis and optimization of sandwich tubes energy absorbers under lateral loading, International Journal of Impact Engineering, 82 (2015) 74-88.

[47] J.O. Hallquist, LS-DYNA theory manual, Livermore software Technology corporation, 3 (2006).

[48] H. Li, W. Chen, H. Hao, Influence of drop weight geometry and interlayer on impact behavior of RC beams, International Journal of Impact Engineering, 131 (2019) 222-237.

[49] H.Y. Jeong, S.C. An, I.C. Seo, E. Lee, S. Ha, N. Kim, Y.C. Jun, 3D printing of twisting and rotational bistable structures with tuning elements, Sci Rep, 9 (2019) 324.

[50] F. Pan, Y. Li, Z. Li, J. Yang, B. Liu, Y. Chen, 3D Pixel Mechanical Metamaterials, Adv Mater, 31 (2019) e1900548.

[51] H. Fang, K.W. Wang, S. Li, Asymmetric energy barrier and mechanical diode effect from folding multi-stable stacked-origami, Extreme Mechanics Letters, 17 (2017) 7-15.